Hematite-ilmenite (Fe₂O₃-FeTiO₃) solid solutions: The effects of cation ordering on the thermodynamics of mixing

NANCY E. BROWN,* ALEXANDRA NAVROTSKY

Department of Geological and Geophysical Sciences, Princeton University, Guyot Hall, Princeton, New Jersey 08544-1003, U.S.A.

ABSTRACT

Enthalpies of reaction from lead borate drop solution calorimetry at 1057 K show that endothermic mixing dominates hematite-ilmenite solid solutions with compositions from $x_{ilm} = 0$ to 0.65, whereas exothermic mixing dominates the compositional region from $x_{ilm} = 0.65$ to 1. The measured enthalpy of mixing is interpreted as arising from two contributions: a positive enthalpy of mixing due to repulsive interaction energies (presumably within a hexagonal layer) and a negative enthalpy of mixing due to attractive interaction energies between layers (i.e., the driving force for ordering).

Enthalpies of reaction have also been measured on compositions from $x_{ilm} = 0.6$ to 0.85 that have different measured cation distributions. Within the resolution of the measurements (± 3 kJ/mol), the enthalpies of isocompositional samples with varying cation distributions are indistinguishable. This observation supports significant short-range order. As the driving force for ordering increases with increasing ilmenite content, progression from short-range order in the more Ti-poor solid solutions to long-range order in the Ti-rich compositions occurs. The progression from short-range to long-range order is expressed by increasingly negative enthalpies of mixing.

Free energies of mixing have been determined independently from the measured tie lines between nonstoichiometric spinel and the sesquioxide phase at 1573 K. This requires modeling the activity of Fe⅔O₄ in the nonstoichiometric spinel solid solutions coexisting with hematite-ilmenite solid solutions. Combination of these free energies of mixing and the experimentally determined enthalpies of mixing suggest that the entropy of mixing is far less positive than that predicted by the maximum configurational entropy implied by the measured site occupancies. These results also support significant short-range order.

INTRODUCTION

Iron titanium oxides of the Fe₂O₃-FeTiO₃ solid solution series impact the evolution of igneous and metamorphic rocks because of the large number of subsolidus equilibria in which they are involved (Haggerty, 1976). Their ubiquitous occurrence with Fe₃O₄-Fe₂TiO₄ solid solutions allows petrologists to estimate the temperature and f_{O_2} conditions under which these mineral assemblages formed. In the classical approach for determining equilibrium T and f_{O_2} conditions, activity-composition relations of Fe₃O₄-Fe₂TiO₄ and Fe₂O₃-FeTiO₃ solid solutions are approximated by subregular solution (Margules) formalisms. Data for selected chemical equilibrium reactions at a number of temperatures, including ilmenite-hematite and magnetite-ulvöspinel pairs, are then used to determine empirically the Margules parameters (Powell and Powell, 1977; Buddington and Lindsley, 1964; Spencer and Lindsley, 1981; Andersen and Lindsley, 1988; Ghiorso, 1990).

Because of the empirical nature of this approach, the most common complications affecting the thermodynamic properties of these solid solutions are ignored. These complications include cation ordering in both Fe₃O₄-Fe₂TiO₄ and Fe₂O₃-FeTiO₃ solid solutions, nonstoichiometry in Fe₃O₄-Fe₂TiO₄ solid solution at $T > 1173$ K (Taylor, 1964; Schmalzried, 1983; Webster and Bright, 1961; Senderov et al., 1993), and chemical impurities. Thus, the calculated parameters have little physical meaning with regard to the atomic interactions that cause macroscopic thermodynamic properties to vary as a function of P, T, and X. The most rigorous attempt to include the effects of cation ordering within the constraints of a simple chemical model has been made by Ghiorso (1990). His results show the importance of including such behavior.

Microscopically based models, on the other hand, take into account the apparently cooperative and higher order nature of the order-disorder process. The most general of such approaches invokes the cluster variation method (CVM), in which interactions out to several nearest neighbors are considered (Burton and Davidson, 1988; Burton, 1985; Burton, 1984; Burton and Kikuchi, 1984; Kikuchi, 1977). In this way, structural and thermodynamic parameters are linked rigorously to the free ener-

* Present address: Norton Company, 1 New Bond Street MS420-601, Worcester, Massachusetts 01615-0008, U.S.A.

TABLE 1. Site-occupancy data for specified compositions and annealing temperatures

Annealing T (K)	Mole fraction FeTiO$_3$	$N_{Ti^{4+},B}$	$N_{Fe^{2+},B}$	$N_{Fe^{3+},B}$	$N_{Ti^{4+},A}$	$N_{Fe^{2+},A}$	$N_{Fe^{3+},A}$
1573	0.8630	0.698	0.166	0.137	0.166	0.698	0.137
1126	0.8570	0.677	0.180	0.143	0.180	0.677	0.143
977	0.8595	0.691	0.169	0.140	0.169	0.691	0.140
1573	0.7001	0.536	0.164	0.300	0.164	0.536	0.300
1273	0.7023	0.574	0.128	0.298	0.128	0.574	0.298
1023	0.7029	0.586	0.120	0.297	0.120	0.586	0.297
1573	0.6094	0.311	0.299	0.391	0.299	0.311	0.391
1073	0.5993	0.406	0.194	0.401	0.194	0.406	0.401
998	0.6013	0.467	0.135	0.399	0.135	0.467	0.399
923	0.5929	0.493	0.100	0.407	0.100	0.493	0.407
1573	0.4080	0.206	0.202	0.593	0.202	0.206	0.593
1573	0.2024	0.102	0.097	0.802	0.097	0.102	0.802

Note: errors in site occupancies range from ±0.01 to +0.024. They have been determined by including the errors arising from the linear extrapolations of the J_s vs. T data to 0 K and the 1 mol% errors in composition. Data are from Brown et al. (1993).

gies of mixing. There are, however, two drawbacks to these types of models. The first is that they are mathematically cumbersome and do not lead to closed-form equations for the mixing parameters. The second is that their energetic parameters cannot be uniquely evaluated from phase equilibria alone, and other direct estimates of the energetics of ordering are not available.

Thus, a major gap remains between the two approaches. The formalism based on simple polynomials and empirical calibration, though petrologically useful, is hard to reconcile with the microscopic complexity of order-disorder and may lead to difficulties when extrapolating outside the P, T, and X range of its determination. The microscopic approach, without more detailed structural and energetic data to constrain its parameters, remains more a conceptual framework than a useful description. This work is a first step in bridging that gap.

In a previous paper (Brown et al., 1993), we reported the preparation and magnetic characterization of a series of ilmenite-hematite solid solutions, which leads to a description of the degree of long-range order of quenched samples. This work reports a drop-solution calorimetric study of the same samples, which provides enthalpies of mixing at room temperature of the same quenched samples. Combination of the structural and calorimetric data with phase equilibrium studies leads to insights into the short- and long-range atomic interactions that affect the thermodynamic mixing properties of hematite-ilmenite solid solutions.

PROCEDURES

Samples

The phases used in this calorimetric study spanned the FeTiO$_3$-Fe$_2$O$_3$ solid solution series in composition and were synthesized under a controlled atmosphere at 1573 K. Relevant compositions (i.e., solid solutions with compositions from $x_{ilm} = 0.6$ to 0.85, where x_{ilm} = mole fraction FeTiO$_3$) were annealed at various temperatures below the order-disorder transition to vary their cation distributions. The composition of each phase at each annealing temperature was determined by WDS microprobe analyses, lattice parameters, and wet chemical analyses. The results showed the compositions to be accurate to within ±1.0 mol%. The saturation magnetization extrapolated to 0 K was used to determine cation distributions for each annealing temperature (Table 1). More detailed discussion of the synthesis and analysis procedures can be found in Brown et al. (1993).

Calorimetric protocol

The purpose of the calorimetric study was to devise a thermodynamic protocol that converted a sample of known structure and oxidation state into a well-defined dissolved final state in the lead borate solvent commonly used for oxide-melt solution calorimetry (Navrotsky, 1977). Because both the degree of order and oxidation can change rapidly in the solid phase at high temperature, the starting state was taken as the sample at room temperature, which was then dropped directly into the solvent at high temperature. In such a drop-solution calorimetric experiment, the total measured enthalpy contains contributions from heat content, dissolution, and any oxidation or reduction in the solvent. No high-temperature equilibration is required, and thus the ambiguity of the samples' oxidation state prior to dissolution is eliminated.

The appropriate calorimetric solvent was determined from preliminary drop-solution experiments with ilmenite in three solvents: sodium molybdate (Navrotsky, 1977); alkali borate (Takayama-Muromachi and Navrotsky, 1988); and lead borate (Navrotsky, 1977). The sodium molybdate solvent showed incomplete dissolution after 120 min at 973 K. The alkali borate solvent showed precipitation of a sodium titanate by optical examinations and X-ray powder diffraction. Experiments in lead borate at 1057 K showed complete dissolution, and X-ray powder diffraction and optical examinations indicated no PbTiO$_3$ precipitation, which had been a problem in earlier experiments using TiO$_2$ at 973 K (Navrotsky, 1977).

The final state of Fe after dissolution in 2PbO-B$_2$O$_3$ solvent was determined by weight gain experiments with solid solutions and mechanical mixtures having compositions between Fe$_2$O$_3$ (all Fe^{3+}) and FeTiO$_3$ (all Fe^{2+}) under conditions of both static air and flowing Ar. The Ar was purified by passing the gas through a Ti purifier (R. D. Mathis GP-100 inert gas purifier) that has been shown to produce an f_{O_2} of $<10^{-6}$. Each weight gain experiment was carried out under conditions that mimic the calorimetric experiments as closely as possible. The following precautions were taken: the surface area of the melt-air interface was kept the same; sample to solvent ratios were restricted to the same range as for a series of calorimetric experiments; experiment durations were 90 min for experiments in air and 70 min for experiments under flowing Ar (as in calorimetry); sample mass was maintained within the same range as that used in the

calorimetric experiments (5–15 mg); and temperature was kept at the calorimeter temperature of 1057 K. Pt crucibles containing lead borate solvent were brought to constant weight at 1057 K under the appropriate atmospheric conditions. Samples were also brought to constant weight at 383 K and ranged from well sintered to poorly sintered.

Figure 1 shows the percent weight gain vs. composition for all experiments. The dashed line indicates the calculated weight gain anticipated for complete oxidation of Fe^{2+} to Fe^{3+} in the solvent for each composition across the solid solution series. The percent of oxidation of Fe^{2+} to Fe^{3+} in the solvent is then calculated relative to this maximum weight gain line. Each data point represents one dissolution experiment, and the error bars represent the propagated cumulative weighing errors ($\sim \pm 0.06$ mg).

For the solid solution experiments conducted in static air (solid circles in Fig. 1), the total range in the calculated percent oxidation lies between 71 and 93%, with the majority of experiments falling between 84 and 93%. Much of this variation in the calculated percent oxidation arises from the extreme sensitivity of this percentage to very small (± 0.01 mg) cumulative weighing errors (e.g., $\sim \pm 6\%$ at $x_{ilm} = 0.2$; $\sim \pm 1.5\%$ at $x_{ilm} = 0.85$). A line fitted to the static air data for compositions between $x_{ilm} = 0.2$ and 0.85 indicates that, after a 90 min experiment, $88 \pm 5.2\%$ of the Fe^{2+} in the sample oxidizes to Fe^{3+}. For solid solutions with $x_{ilm} \geq 0.85$, however, the degree of oxidation does not reach this limit in 90 min. For ilmenite, the percent oxidation reached after 90 min is only $\sim 65\%$. By ~ 300 min, the percent oxidation reached $\sim 88\%$. We infer from this that the oxidation process is controlled by the diffusion of O into the lead borate solvent at the solvent-air interface. Similar conclusions were reached by Zhou et al. (1993) for the $Cu^+ \rightarrow Cu^{2+}$ reaction.

Mechanical mixtures (open circles in Fig. 1) of hematite and ilmenite indicate a final oxidation state reflecting a weighted average of the oxidation states of the two end-members. The difference between the final oxidation state of ilmenite (i.e., 65% oxidation of Fe^{2+} to Fe^{3+} after 90 min) and that for solid solution with $x_{ilm} < 0.85$ (i.e., 88% oxidation of Fe^{2+} to Fe^{3+} after 90 min) causes the final oxidation state for the mechanical mixture to be different from that for solid solutions. Thus the amount of oxidation occurring during a calorimetric experiment is not the same for solid solutions and mechanical mixtures, making interpretation of the calorimetric results from experiments in static air dependent on the enthalpy of oxidation. For solid solutions of a different composition, there is no inherent reason why this enthalpy of oxidation should be constant for all compositions, and the large errors associated with the amount of oxidation determined by weight gain analysis results in uncertainties in the enthalpy of oxidation of ~ 15–20%.

The experiments in Ar (solid stars in Fig. 1), on the other hand, show no change in weight for all compositions across the solid solution series after 70 min. However, this is only true when the lead borate solvent has
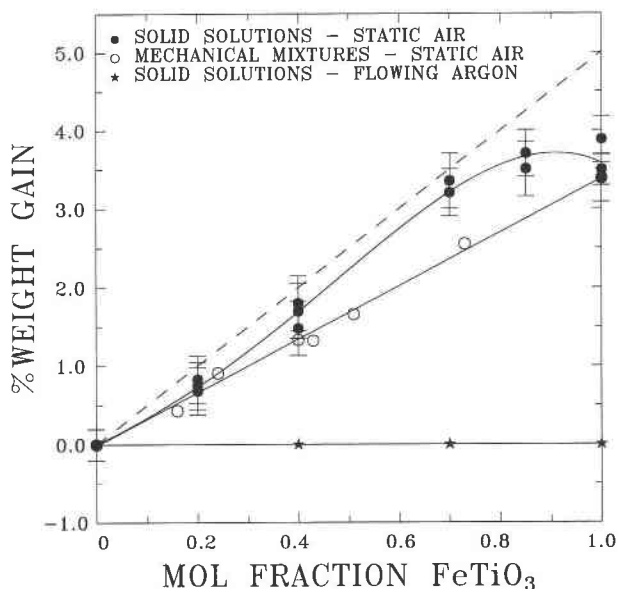

Fig. 1. Percent weight gained in lead borate solvent at 1057 K because of oxidation of Fe_2O_3-$FeTiO_3$ solid solutions and mechanical mixtures. The dashed line represents the percent weight gain expected for complete oxidation of Fe^{2+} to Fe^{3+} in the solvent. The solid circles represent 90-min experiments with Fe_2O_3-$FeTiO_3$ solid solutions in static air. The open circles represent 90-min experiments with mechanical mixtures of Fe_2O_3 and $FeTiO_3$ in static air. The solid stars represent 70-min experiments with Fe_2O_3-$FeTiO_3$ solid solutions in flowing Ar.

been equilibrated for ~ 15 h under flowing Ar at the calorimeter temperature prior to dissolution of the samples. Calorimetric experiments conducted without this equilibration time show small parasitic exothermic reactions and a very slow return to the base line, suggesting that the sample was oxidized slowly. This suggests that there is a small solubility of O in the solvent in equilibrium with air that is greatly reduced when the solvent is equilibrated with flowing Ar. Once this O is removed from the solvent, no oxidation or reduction of Fe in the solvent occurs during the calorimetric experiment.

As a result of the above considerations, drop-solution calorimetric experiments were completed in a Calvet-type microcalorimeter (Navrotsky, 1977) at 1057 K in 2PbO-B_2O_3 solvent under conditions of flowing Ar, with overnight preequilibration of the solvent under Ar gas flow. Each experiment was 70 min in length. Solid solution experiments involved dropping small chunks (7–25 mg) of Fe_2O_3-$FeTiO_3$ solid solutions. Mechanical mixture experiments involved dropping two small chunks of the end-members together. This procedure eliminated the extra heat effect attributable to any capsule. The samples dissolved rapidly and completely. The high temperature (1057 instead of 973 K) and intimate contact of the dropped sample with the solvent (no Pt sample capsule) may have aided rapid dissolution and avoided local $PbTiO_3$ saturation.

TABLE 2. Drop-solution reaction enthalpies at 1057 K in lead borate solvent under conditions of flowing Ar for solid solutions and mechanical mixtures

	Solid solutions		Mechanical mixtures	
Anneal-ing T (K)	Mole fraction $FeTiO_3$	Total H (kJ/mol)	Mole fraction $FeTiO_3$	Total H^* (kJ/mol)
1573	0	177.1 ± 2.5(5)** †	0.0800	176.5
1573	0.1985	166.0 ± 4.3(5)	0.2758	170.6
1573	0.4068	158.0 ± 4.2(5)	0.4653	165.9
1573	0.6094	157.5 ± 3.5(5)	0.5648	161.8
1073	0.5993	157.7 ± 3.3(5)	0.8905	156.5
998	0.6013	156.2 ± 3.0(5)		
1573	0.7001	160.1 ± 2.7(5)		
1273	0.7023	158.1 ± 4.2(5)		
1023	0.7029	162.8 ± 4.1(5)		
1126	0.8570	157.4 ± 0.4(5)		
977	0.8595	157.4 ± 2.6(5)		
1338	1	148.9 ± 3.4(5)		

* No errors are indicated for the mechanical mixtures because each value represents one experiment in which a chunk of both Fe_2O_3 and $FeTiO_3$ were dropped simultaneously. Thus, compositions are calculated from the relative weights of each chunk.

** Error represents 2 sd of the mean.

† Number in parentheses indicates the number of experiments.

CALORIMETRIC RESULTS

Observed enthalpies

The enthalpies of the drop solution of mechanical mixtures and Fe_2O_3-$FeTiO_3$ solid solutions with varying compositions and degrees of cation order are listed in Table 2. For compositions from $x_{ilm} = 0.6$ to 0.85 with differing cation distribution, no measurable difference in reaction enthalpy was found for isocompositional samples (Table 2); hence, only the average values are plotted in Figure 2. Excess enthalpies are determined by subtracting the measured enthalpies of the solid solutions from those of the mechanical mixtures. This difference represents the enthalpy of mixing at 298 K of solid solutions having a structural state assumed to be characteristic of their quench temperatures. The enthalpies of disordering are determined by subtracting the total measured enthalpies for two solid solutions of the same composition but with differing thermal histories.

Enthalpies of mixing

Excess enthalpies for each solid solution are shown in Figure 3. Solid solutions with compositions from $x_{ilm} = 0$ to 0.65 show endothermic enthalpies of mixing, whereas solid solutions with compositions from $x_{ilm} = 0.65$ to 1 show exothermic enthalpies of mixing. These results are consistent with the model of Burton and Davidson (1988), which incorporates dominantly positive (i.e., repulsive) intralayer Fe^{2+}-Ti^{4+} interactions in hematite-rich solid solutions and dominantly negative (i.e., attractive, ordering) interlayer Fe^{2+}-Ti^{4+} interactions in ilmenite-rich solid solutions. However, other interpretations are not ruled out; e.g., size effects result in the repulsive forces that drive phase separation, whereas attractive interlayer forces drive ordering. The data obtained can be used to
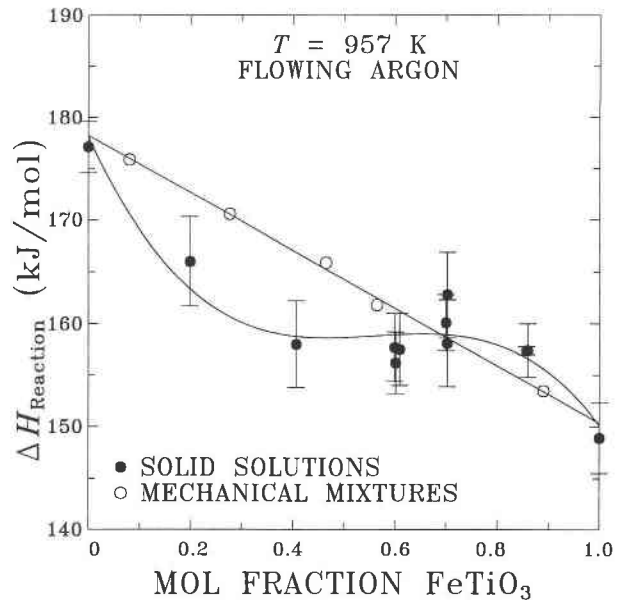

Fig. 2. Reaction enthalpy (kJ/mol) from drop-solution experiments at 1057 K in flowing Ar vs. mole fraction ilmenite. The open circles represent the reaction enthalpies for individual experiments with mechanical mixtures of ilmenite and hematite, and the solid circles represent the reaction enthalpies measured for the Fe_2O_3-$FeTiO_3$ solid solutions. The reaction enthalpy includes contributions from the heat content and dissolution. The error bars represent 2 sd of the mean.

constrain parameters in microscopically based models such as CVM, but doing so is beyond the scope of this paper.

The data can be fitted by a subregular (two-parameter) solution model

$$\Delta H_{mix} = x_{ilm}(1 - x_{ilm})(79.3788 - 120.843x_{ilm}). \quad (1)$$

The change in sign in the enthalpy of mixing is reflected in the opposite signs of the two parameters. We stress that the above polynomial, though convenient, has little physical significance because of the complex variation of both short- and long-range order with composition and temperature (see below).

Enthalpies of disordering

In order to measure the enthalpy of disordering, compositions for $x_{ilm} = 0.6$ to 0.85 were annealed at temperatures below the order-disorder transition and their cation distributions measured (Table 1 of this paper; Brown et al., 1993). The order parameter determined from saturation magnetization measurements, Q_M, varies directly with the crystallographic site occupancies of Ti^{4+}, Fe^{3+}, and Fe^{2+}. From a crystallographic perspective, the three cations would be distributed over the A and B sublattices such that charge balance over the structure would be maintained and cation to cation repulsion across the shared octahedral face would be minimized. Minimization of the highly repulsive Ti^{4+}-Ti^{4+} pairs in both or-
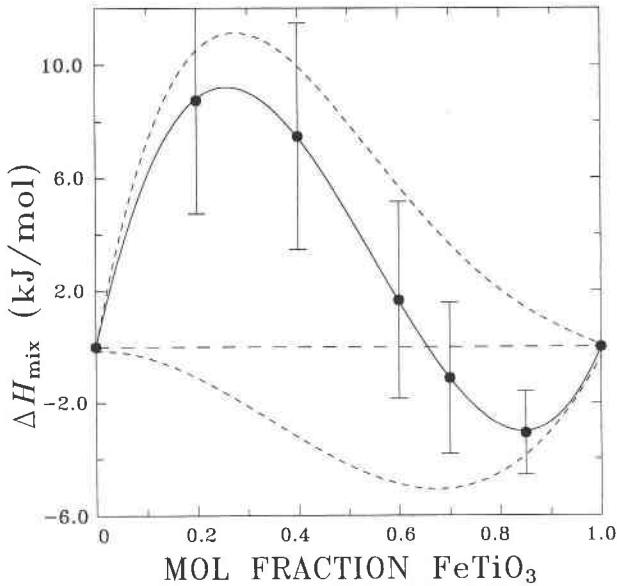
Fig. 3. Enthalpies of mixing at 1057 K for Fe_2O_3-$FeTiO_3$ solid solutions (solid circles) calculated from the fit to the data in Fig. 2 and Table 3. The error bars represent the propagated 2 sd of the mean. The line with long dashes represents ideal behavior. The curves with short dashes represent one set of positive (upper dashed curve) and negative (lower dashed curve) enthalpies of mixing (see text) that would sum to give the measured enthalpies of mixing.

TABLE 3. Entropies of mixing calculated with $S_{conf,ilm} = 3.3$ J/(mol·K) and $S_{conf,ilm} = 0$ J/(mol·K) for the Fe_2O_3-$FeTiO_3$ solid solutions

Anneal-ing T (K)	Mole fraction $FeTiO_3$	ΔS_{mix}* [J/(mol·K)]	ΔS_{mix}** [J/(mol·K)]	Q_{M_s}
1338	1.0000	0	0	1.000
1573	0.8630	10.81(63)†	13.66(63)	0.616
1126	0.8570	11.32(56)	14.15(56)	0.580
977	0.8595	10.98(61)	13.82(61)	0.607
1573	0.7001	14.18(51)	16.49(51)	0.531
1273	0.7023	13.36(64)	15.67(64)	0.635
1023	0.7029	13.11(75)	15.43(75)	0.660
1573	0.6094	16.14(50)	18.15(50)	0.020
1073	0.5993	15.49(34)	17.47(34)	0.353
998	0.6013	14.53(56)	16.50(56)	0.558
923	0.5929	13.75(70)	15.71(70)	0.663
1573	0.4084	14.59(55)	15.94(55)	0.005
1573	0.2024	9.91(27)	10.58(27)	0

* The ΔS_{mix} calculated with $S_{conf,ilm} = 3.3$ J/(mol·K).
** The ΔS_{mix} calculated with $S_{conf,ilm} = 0$ J/(mol·K).
† The errors represent the uncertainty in $S_{conf,ss}$, calculated assuming the maximum error (i.e., 0.024) in the Ti site-occupancy data, adjusting the other site occupancies according to compositional constraints, and assuming that Fe^{3+} is distributed equally on the A and B sublattices (see text for discussion).

dered and disordered solid solutions of all compositions occurs when Fe^{3+} is distributed equally in the A and B sites. Therefore, assuming that Fe^{3+} is equally distributed over both sublattices, we need only be concerned with the ordering of Fe^{2+} and Ti^{4+} on the A and B sublattices. The order parameter, Q_{M_s}, is related to the site occupancies by the general definition

$$Q_{M_s} = (X_{Fe^{2+},A} - X_{Fe^{2+},B})/(X_{Fe^{2+},A} + X_{Fe^{2+},B})$$

$$= (X_{Ti^{4+},A} - X_{Ti^{4+},B})/(X_{Ti^{4+},A} + X_{Ti^{4+},B}) \quad (2)$$

where $X_{Fe^{2+},A}$ is the sublattice mole fraction of Fe^{2+} in the A sublattice (Brown et al., 1993).

Table 3 shows that as the composition approaches ilmenite, the range in the order parameter for different annealing temperatures becomes smaller (i.e., for composition with $x_{ilm} = 0.6$ the order parameter varies from 0 to 0.66, for $x_{ilm} = 0.7$ it varies from 0.53 to 0.66, and for $x_{ilm} = 0.85$ the range is only 0.58 to 0.61). This decrease in variation of the order parameter as compositions become more ilmenite rich suggests that the high-temperature disordered state becomes from difficult to quench (Brown et al., 1993).

Enthalpies of drop solution (Table 2) measured on these samples are indistinguishable within the resolution of the calorimetric experiments (± 3 kJ/mol). These results suggest that significant differences in the cation distributions in this compositional range do not result in significant enthalpy changes. This is permissible if short-range order

dominates and supports our interpretation of the change in sign of the enthalpy of mixing curve (above). Thus, short-range order is suggested by both the increasingly negative enthalpies of mixing in the intermediate compositional range and the insignificant enthalpy changes for compositions with large changes in degree of long-range order (e.g., $x_{ilm} = 0.6$). As long-range order begins to dominate (close to ilmenite compositions), the enthalpy of mixing becomes exothermic.

CALCULATIONS FROM PHASE EQUILIBRIA

The purpose of this section is to estimate free energies of mixing in hematite-ilmenite solid solutions for the equilibrium between sesquioxide and spinel phases. These free energies are then combined with our measured enthalpies of mixing to estimate entropies of mixing in hematite-ilmenite solid solutions and to provide evidence for the diminution of configurational entropy due to both short- and long-range order.

NONSTOICHIOMETRIC SPINEL SOLID SOLUTIONS

Calculation of activity and free energy of transformation of $Fe_{8/3}O_4$ (α-γ)

The data of Taylor (1964) showed that at 1573 K a significant range of nonstoichiometry exists in the ulvö-spinel-magnetite solid solution series (dashed line in Fig. 4). Schmalzried (1983) has investigated the range in nonstoichiometry in Fe_3O_4 at temperatures between 1173 and 1673 K. His results are listed in Table 4 in terms of mole fraction $Fe_{8/3}O_4$ and Fe_3O_4. Combining the data of Taylor (1964) and Schmalzried (1983), the limit of nonstoichiometry for Fe_3O_4-Fe_2TiO_4 solid solutions has been estimated (dashed line in Fig. 4) and used to estimate the compositions of the nonstoichiometric spinel solid solu-
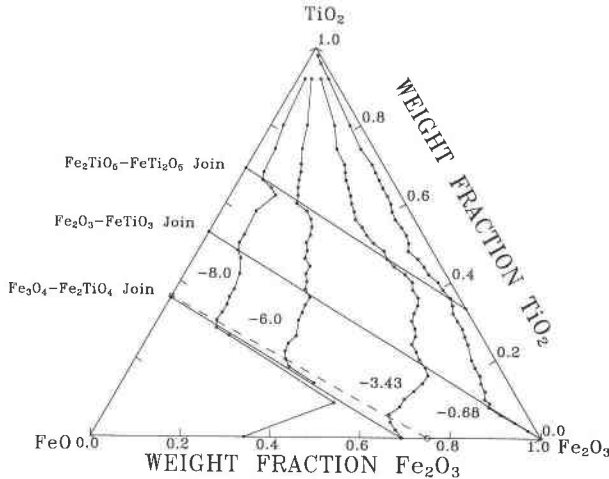
Fig. 4. Ternary phase diagram for the FeO-TiO₂-Fe₂O₃ system (modified from Taylor, 1964). The composition in weight fraction oxides (solid circles) is plotted for each of four log f_{O_2} (−0.68, −3.43, −6.0, −8.0) from the experimental data of Taylor (1964). The dashed line represents the limit of nonstoichiometry in the spinel solid solutions assumed in our model (see text). The open circle represents the composition of Fe₃O₄ in equilibrium with Fe₂O₃ at 1573 K from Schmalzried (1983). The Fe₂TiO₅-FeTi₂O₅, Fe₂O₃-FeTiO₃, and Fe₃O₄-Fe₂TiO₄ joins are shown for reference.

TABLE 4. Solubility data for $Fe_{8/3}O_4$ in Fe₃O₄ coexisting with Fe₂O₃ at temperatures between 1173 and 1573

T (K)	O/Fe*	x_{Fe}	$x_{Fe_3O_4}$**	$x_{Fe_{8/3}O_4}$
1573	1.364	2.932	0.795	0.205
1473	1.357	2.948	0.845	0.155
1373	1.349	2.966	0.899	0.101
1273	1.341	2.981	0.947	0.053
1173	1.337	2.992	0.974	0.026

* Estimated from Fig. 4 in Schmalzried (1983).
** Calculated as
$$[x_{Fe_3O_4(mag)} - x_{Fe_3O_4(Fe_{8/3}O_4)}]/[x_{Fe(mag)} - x_{Fe(Fe_{8/3}O_4)}] = 100/0.333 = 300.003$$
$$300.003(\Delta x_{Fe, \text{ at } T(K)}) = \Delta x_{Fe_3O_4, \text{ at } T(K)}$$
where $x_{Fe_3O_4(mag)}$ (= 100) and $x_{Fe_3O_4(Fe_{8/3}O_4)}$ (= 0) are the mole fractions of Fe₃O₄ in pure Fe₃O₄ and pure $Fe_{8/3}O_4$, respectively. The $\Delta x_{Fe(mag)}$ and $\Delta x_{Fe(Fe_{8/3}O_4)}$ are the mole fractions of Fe in pure Fe₃O₄ and pure $Fe_{8/3}O_4$, respectively.

tions coexisting with ilmenite-hematite solid solutions (Table 5). These results are in good agreement with the oxidation boundary calculated by Aragón and McCallister (1982). If enough f_{O_2} data were distributed in the Fe-Ti-O ternary, one could calculate the activities of all oxide components by appropriate ternary Gibbs-Duhem integrations. After several attempts in this direction, we concluded that the data are too sparse at any one temperature for a meaningful calculation independent of simplifying assumptions. We chose to apply a simple mixing model to the spinel solid solutions. We could then utilize the coexisting pairs at 1573 K (our data and those of Taylor, 1964) to determine activity-composition relations along the pseudobinary Fe₂O₃-FeTiO₃ join. Our approach to calculating the free energies of mixing in both the titanomagnetite and hematite-ilmenite solid solution series differs from that of Aragón and McCallister (1982) in two respects. For the titanomagnetite series, we have both assumed athermal mixing; however, Aragón and McCallister assumed mixing over only one site. In our model, we have taken into account cation ordering (i.e., mixing over two sites). In addition, their approach for the hematite-ilmenite series was to assume a simple mixing model for the excess free energies. In our model, we make no assumptions for the free energies of mixing in the hematite-ilmenite solid solution series (see below).

With the assumption that mixing in γ-$Fe_{8/3}O_4$-Fe₂TiO₄-Fe₃O₄ solid solutions is athermal and governed by the configurational entropy, it is possible to calculate the

change in free energy relative to hematite (Fe₂O₃ = α-$Fe_{8/3}O_4$), magnetite (Fe₃O₄), and ulvöspinel (Fe₂TiO₄) as

$$\Delta G_{ss} = y\Delta G_{trans}(\alpha\text{-}\gamma) + \Delta G_{mix} \tag{3}$$

where y is the mole fraction of γ-$Fe_{8/3}O_4$ in the ternary spinel solid solution and $\Delta G_{trans}(\alpha\text{-}\gamma)$ is the free energy of transformation for the reaction

$$\alpha\text{-}Fe_{8/3}O_4 = \gamma\text{-}Fe_{8/3}O_4. \tag{4}$$
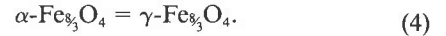
This transformation free energy can be calculated from the binary solid solubility data of Schmalzried (1983) (Table 4). For an $Fe_{8/3}O_4$-saturated magnetite phase coexisting with hematite, $\mu_{Fe_{8/3}O_4}$ must be equal in both phases at equilibrium. In hematite, $\mu_{Fe_{8/3}O_4}$ is the free energy of formation per four O atoms mole of Fe₂O₃. In the saturated γ phase,

$$\mu_{Fe_{8/3}O_4} = \mu^0_{Fe_{8/3}O_4,\gamma} + RT \ln a_{Fe_{8/3}O_4,\gamma} \tag{5}$$

where

$$\mu^0_{Fe_{8/3}O_4,\gamma} = \mu^0_{Fe_{8/3}O_4,\alpha} + \Delta G_{trans}(\alpha\text{-}\gamma). \tag{6}$$

At equilibrium, this gives

$$\Delta G_{trans}(\alpha\text{-}\gamma) = -RT \ln a_{Fe_{8/3}O_4,\gamma} \tag{7}$$

where

$$RT \ln a_{Fe_{8/3}O_4,\gamma} = -T\Delta \bar{s}_{Fe_{8/3}O_4,\gamma}. \tag{8}$$

In this equation, $\Delta \bar{s}_{Fe_{8/3}O_4}$ is the partial molar entropy of $Fe_{8/3}O_4$ in the γ phase (see below). Computation yields a value for $\Delta G_{trans}(\alpha\text{-}\gamma) = 14.6 \pm 0.6$ kJ/mol. The error in ΔG_{trans} has been calculated assuming a compositional error of 2 mol% $Fe_{8/3}O_4$ in the solubility data of Schmalzried (1983) (Table 4). These data can also be used to estimate the enthalpy and entropy of the transition ΔH_{trans} and ΔS_{trans}, respectively, where

$$\partial \Delta G_{trans}/\partial T = -\Delta S_{trans}. \tag{9}$$

The ΔG_{trans} is calculated as described above. The transition temperature where pure α-$Fe_{8/3}O_4$ transforms to pure

TABLE 5. Compositions of the nonstoichiometric spinel solid solutions and coexisting ilmenite-hematite solid solutions estimated from Taylor (1964)

	Ilmenite-hematite solid solution		Nonstoichiometric spinel solid solution		
In f_{O_2}	Mole fraction $FeTiO_3$	Mole fraction Fe_2O_3	Mole fraction Fe_3O_4	Mole fraction Fe_2TiO_4	Mole fraction $Fe_{8/3}O_4$
−25.33	0.982	0.018	0.009	0.976	0.015
−23.03	0.957	0.043	0.038	0.930	0.032
−20.72	0.923	0.077	0.074	0.886	0.040
−18.42	0.887	0.113	0.125	0.822	0.053
−16.12	0.828	0.172	0.209	0.722	0.070
−14.97	0.751	0.249	0.269	0.648	0.083
−13.82	0.701	0.299	0.334	0.564	0.102
−11.51	0.547	0.453	0.501	0.361	0.138
−7.90	0.333	0.667	0.664	0.157	0.179
−3.71	0	1.000	0.796	—	0.204

Note: converted from weight fraction FeO, TiO_2, and Fe_2O_3 (from Taylor, 1964).

TABLE 6. Values of $a_{Fe_{8/3}O_4,\gamma}$, $a_{Fe_{8/3}O_4,\alpha}$, a_{hem}, and a_{ilm} calculated for the coexisting nonstoichiometric spinel and ilmenite-hematite solid solutions, as discussed in the text

In f_{O_2}	$a_{Fe_{8/3}O_4,\gamma}$	$a_{Fe_{8/3}O_4,\alpha}$	a_{hem}	a_{ilm}
−25.33	9.10×10^{-6}	2.8×10^{-5}	4.0×10^{-4}	0.9639
−23.03	1.79×10^{-4}	5.5×10^{-4}	3.6×10^{-3}	0.9003
−20.72	6.52×10^{-4}	2.0×10^{-3}	9.5×10^{-3}	0.8462
−18.42	2.25×10^{-3}	6.9×10^{-3}	2.4×10^{-2}	0.7711
−16.12	7.88×10^{-3}	2.4×10^{-2}	6.1×10^{-2}	0.6642
−14.97	1.53×10^{-2}	4.7×10^{-2}	0.100	0.5844
−13.82	2.90×10^{-2}	8.9×10^{-2}	0.163	0.4869
−11.51	8.75×10^{-2}	0.268	0.371	0.2930
−7.90	0.199	0.611	0.691	0.1453
−3.71	0.326	1.000	1.000	0

γ-$Fe_{8/3}O_4$ can be estimated by extrapolating the Fe_3O_4-$Fe_{8/3}O_4$ solid solubility data (Table 4) to pure γ-$Fe_{8/3}O_4$. It is important to remember, however, that the limit of the solubility data is 0.205 mole fraction $Fe_{8/3}O_4$. Thus, the extrapolated temperature of 3135 K must be taken with caution. In any case, it is above the actual decomposition and melting temperatures. This transition temperature can be combined with the transition entropy determined by Equation 9 at equilibrium where

$$\Delta H_{trans} = T \Delta S_{trans}. \quad (10)$$

Values of ΔH_{trans} and ΔS_{trans} are 36.1 kJ/mol and 11.5 J/(mol·K), respectively. The free energy of transition can then be calculated to be 17.9 kJ/mol at 1573 K from these values. This value is in reasonable agreement with the value determined with Equations 7 and 8, when one considers the uncertainty in the transition temperature at pure $Fe_{8/3}O_4$. Because of this uncertainty, we have chosen to use the value determined from Equations 7 and 8 in the calculations below.

For the Ti-bearing solid solutions,

$$\mu_{Fe_{8/3}O_4,\alpha} = \mu^0_{Fe_{8/3}O_4,\alpha} + RT \ln a_{Fe_{8/3}O_4,\alpha}. \quad (11)$$

Therefore, at equilibrium between a nonstoichiometric spinel solid solution and an ilmenite-hematite solid solution,

$$RT \ln a_{Fe_{8/3}O_4,\alpha} = \Delta G_{trans}(\alpha\text{-}\gamma) + RT \ln a_{Fe_{8/3}O_4,\gamma}. \quad (12)$$

The data of Taylor (1964) were used to estimate the compositions of the nonstoichiometric spinel solid solutions in equilibrium with hematite-ilmenite solid solutions (Table 5). Values for $a_{Fe_{8/3}O_4,\alpha}$ and $a_{Fe_{8/3}O_4,\gamma}$ are listed in Table 6.

Calculations of the entropy of mixing in the spinel phase

Configurational entropies and the correspondingly statistically ideal entropies of mixing for γ-$Fe_{8/3}O_4$-Fe_3O_4-Fe_2TiO_4 solid solutions are calculated as follows. The site occupancies of the end-members are defined as ([ ] = octahedral site, ( ) = tetrahedral site, □ = vacancies):

Fe_3O_4 = random spinel at high temperature
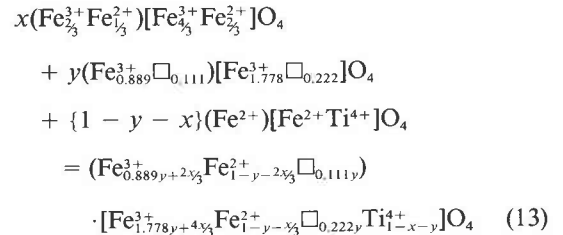
$$(Fe^{3+}_{2/3} Fe^{2+}_{1/3})[Fe^{3+}_{4/3} Fe^{2+}_{2/3}]O_4$$

$Fe_{8/3}O_4$ = random spinel at high temperature

$$(Fe^{3+}_{0.889} \square_{0.111})[Fe^{3+}_{1.778} \square_{0.222}]O_4$$

Fe_2TiO_4 = inverse spinel at high temperature

$$(Fe^{2+})[Fe^{2+}Ti^{4+}]O_4.$$
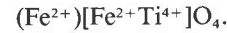
The reaction describing the solid solution can be written as follows, assuming that the solid solution maintains the site preferences of the end-members (i.e., Ti in octahedral site only, □ distributed randomly, etc.)

$$x(Fe^{3+}_{2/3} Fe^{2+}_{1/3})[Fe^{3+}_{4/3} Fe^{2+}_{2/3}]O_4$$
$$+ y(Fe^{3+}_{0.889}\square_{0.111})[Fe^{3+}_{1.778}\square_{0.222}]O_4$$
$$+ \{1 - y - x\}(Fe^{2+})[Fe^{2+}Ti^{4+}]O_4$$
$$= (Fe^{3+}_{0.889y+2x/3}Fe^{2+}_{1-y-2x/3}\square_{0.111y})$$
$$\cdot [Fe^{3+}_{1.778y+4x/3}Fe^{2+}_{1-y-x/3}\square_{0.222y}Ti^{4+}_{1-x-y}]O_4 \quad (13)$$

where x, y, and $(1 - x - y)$ are the mole fractions of Fe_3O_4, $Fe_{8/3}O_4$, and Fe_2TiO_4, respectively. The change in configurational entropy, ΔS_{conf}, for this reaction is given by

$$\Delta S_{conf} = S_{conf,ss} - xS_{conf,Fe_3O_4} - yS_{conf,Fe_{8/3}O_4} - zS_{conf,Fe_2TiO_4} \quad (14)$$

where $z = (1 - x - y)$ and

$$S_{conf,ss} = -R\{(0.889y + 2x/3)\ln(0.889y + 2x/3)$$
$$+ (1 - y - 2x/3)\ln(1 - y - 2x/3)$$
$$+ (0.111y \ln 0.111y)$$
$$+ (1.778y + 4x/3)\ln(1.778y + 4x/3)/2$$
$$+ (1 - y - x/3)\ln(1 - y - x/3)/2$$
$$+ 0.222y \ln 0.111y$$
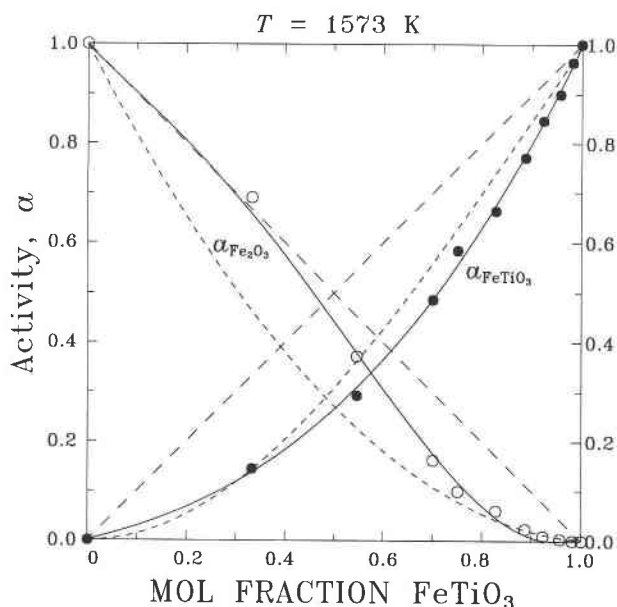$$+ (1 - x - y)\ln(1 - x - y)/2 \quad (15)$$

Fig. 5. Activity-composition relations at 1573 K in Fe_2O_3-$FeTiO_3$ solid solutions. The activity of Fe_2O_3 (open circles and solid curve) has been calculated with our model for nonstoichiometric spinel solid solutions and the data of Taylor (1964) for coexisting spinel and ilmenite solid solutions (see text). The activity of $FeTiO_3$ (solid circles, solid curve) has been calculated by Gibbs-Duhem integration (see text). In addition, the activities of Fe_2O_3 and $FeTiO_3$ (curves with small dashes) have also been calculated from the empirical formulation of Ghiorso (1990). The lines with large dashes indicate the condition $a_i = x_i$, where i is either Fe_2O_3 or $FeTiO_3$.

$$S_{conf,Fe_3O_4} = -R\{2 \ln \tfrac{2}{3} + \ln \tfrac{1}{3}\} \tag{16}$$

$$S_{conf,Fe_2TiO_4} = -R\{2 \ln \tfrac{1}{2}\} \tag{17}$$

$$S_{conf,Fe_{8/3}O_4} = -R\{0.111 \ln 0.111 + 0.889 \ln 0.889$$
$$+ 1.778 \ln 0.889 + 0.222 \ln 0.111\}. \tag{18}$$

By combining terms, this becomes

$$S_{conf} = -R\{0.333y \ln y - (1 - 0.111y - x)\ln 3$$
$$+ (0.889y + \tfrac{2x}{3})\ln(2.667y + 2x)$$
$$+ (1 - y - \tfrac{2x}{3})\ln(3 - 3y - 2x)$$
$$+ (1.778y + \tfrac{4x}{3})\ln(5.334y + 4x)$$
$$+ (1 + 0.778y - x)\ln 6$$
$$+ (1 - y - \tfrac{x}{3})\ln(3 - 3y - x)$$
$$+ (1 - x - y)\ln(1 - x - y)$$
$$+ (1 - \tfrac{7x}{3} - y)\ln 2 - \tfrac{4x}{3} \ln 4$$
$$- 2.667y \ln 0.889\}. \tag{19}$$

This equation can be written in terms of the partial molar entropies as

$$\Delta S_{conf} = x\Delta \bar{s}_{Fe_3O_4} + y\Delta \bar{s}_{Fe_{8/3}O_4} + z\Delta \bar{s}_{Fe_2TiO_4}. \tag{20}$$

This gives

$$S_{conf} = -R\{x[\tfrac{2}{3} \ln(2.667y + 2x) + \tfrac{1}{3} \ln(3 - 3y - 2x)$$
$$+ \tfrac{4}{3} \ln(5.334y + 4x) + \tfrac{2}{3} \ln(3 - 3y - x)$$
$$- \tfrac{4}{3} \ln 2 - \tfrac{4}{3} \ln 4]$$
$$+ y[0.333 \ln y - 0.889 \ln 3$$
$$+ 0.889 \ln(2.667y + 2x)$$
$$+ 1.778 \ln(5.334y + 4x) - 1.778 \ln 6$$
$$- 2.667 \ln 0.889]$$
$$+ z[-\ln 3 + \ln(3 - 3y - 2x)$$
$$- \ln 6 + \ln(3 - 3y - x)$$
$$+ \ln(1 - x - y) + \ln 2]\}. \tag{21}$$

The partial molar entropies can then be written as

$$\Delta \bar{s}_{Fe_3O_4} = -R \ln[(2.667y + 2x)^{2/3}(3 - 3y - 2x)^{1/3}$$
$$\cdot(5.334y + 4x)^{4/3}$$
$$\cdot(3 - 3y - x)^{2/3}(2)^{-4/3}(4)^{-4/3}] \tag{22}$$

$$\Delta \bar{s}_{Fe_{8/3}O_4} = -R \ln[(y)^{0.333}(3)^{-0.889}(2.667y + 2x)^{0.889}$$
$$\cdot(5.334y + 4x)^{1.778}(6)^{-1.778}$$
$$\cdot(0.889)^{-2.667}] \tag{23}$$

$$\Delta \bar{s}_{Fe_2TiO_4} = -R \ln[(3)^{-1}(3 - 3y - 2x)(6)^{-1}$$
$$\cdot(3 - 3y - x)(1 - x - y)(2)]. \tag{24}$$

We believe that for the high temperature of equilibrium involved (1573 K), the above model, which assumes maximum randomness and only $^{[6]}Ti^{4+}$, is a good approximation. Other models incorporating Fe^{2+}-Fe^{3+} site-preference equilibria (e.g., O'Neill and Navrotsky, 1984) would give slightly different results. In view of the improbability of completely quenching the high-temperature structural state and the ambiguity in even distinguishing Fe^{2+} and Fe^{3+} at high temperature, this simplest model is probably the best approach.

COEXISTING SPINEL-SESQUIOXIDE PAIRS

Activities of Fe_2O_3 and $FeTiO_3$ in the sesquioxide phase

The activity of Fe_2O_3 in the ilmenite-hematite solid solution series, a_{hem}, can be calculated from the activity of $Fe_{8/3}O_4$ in the spinel solid solution series (Eq. 12) and the relation

$$a_{Fe_{8/3}O_4,\alpha} = (a_{hem})^{4/3}. \tag{25}$$

Values for activities of Fe_2O_3 are shown in Table 6 and Figure 5. No polynomial form could be found to fit the activity-composition relations, such that the a-x relations reduce to Raoult's law as the mole fraction approaches 1.0. Such complex behavior is not surprising, since the mixing behavior results from the interplay between negative and positive interactions that will vary as a function of temperature and composition.

The activity of $FeTiO_3$, a_{ilm}, can be calculated by Gibbs-Duhem integration, where

$$\ln a_{ilm} = -\int_{\ln a_{hem}(a_{hem}=0)}^{\ln a_{hem}} (x_{hem}/x_{ilm})d \ln a_{hem}. \quad (26)$$

In this equation, x_{hem} and x_{ilm} are the mole fractions of Fe_2O_3 and $FeTiO_3$, respectively, in the ilmenite solid solution coexisting with the spinel solid solution. The above integration was carried out by plotting x_{hem}/x_{ilm} vs. $\ln a_{hem}$ and fitting these data with exponential equations such that $\ln a_{hem}$ would tend to negative infinity as x_{hem}/x_{ilm} approached zero, and x_{hem}/x_{ilm} would tend to positive infinity as $\ln a_{hem}$ approached one. Calculated results are shown in Figure 5 and Table 6. In addition to the activities calculated from our microscopically based model for the spinel solid solution series, activities calculated using the empirical model of Ghiorso (1990) are also shown for comparison. Both sets of activities show negative deviations from Raoult's Law and agree moderately well with each other. The integral free energies of mixing agree quite well (see below).

The free energies of mixing can be calculated from the activities of Fe_2O_3 and $FeTiO_3$ as

$$\Delta G_{mix} = RT\{x_{ilm}\ln a_{ilm} + (1 - x_{ilm})\ln a_{hem}\} \quad (27)$$

where R is the gas constant, T is the temperature (in K), and a_{ilm} and a_{hem} are the activities of ilmenite and hematite, respectively, determined from our model of the activity of Fe_8O_{13} in the nonstoichiometric spinel solid solution. Values for the free energy of mixing are calculated in Table 7.

ENTROPIES OF MIXING IN Fe_2O_3-$FeTiO_3$

Maximum configurational entropies of mixing from site occupancies

Calculation of the entropies of mixing in the Fe_2O_3-$FeTiO_3$ system requires explicit definition of the configurational entropies in the end-member components. For hematite, this definition is obvious with $S_{conf,hem} = 0$ J/(mol·K). For ilmenite, cation ordering has been studied extensively both in situ at high temperatures and pressures and on samples quenched from high temperatures (e.g., Wechsler and Prewitt, 1984; Shirane et al., 1962). The neutron diffraction data of Shirane et al. (1962) on quenched samples have shown ilmenite to have ($x_{ilm} - x$) = 0.95 [i.e., ($x_{ilm} - x$) = degree of order = sublattice mole fraction Ti in the B site], although no error bars have been given for this result ($S_{conf,ilm} = 3.30$). The diffraction data of Wechsler and Prewitt (1984) have shown that no appreciable disorder occurs at high temperatures ($S_{conf,ilm} = 0$). Our determination of the degree of order in ilmenite from saturation magnetization measurements to 4 K (Brown et al., 1993) agree with the data of Wechsler and Prewitt (1984).

Configurational entropies of the solid solutions can be calculated from measured site occupancies (Table 1), following the formulation of Thompson (1969, 1970)

TABLE 7. Calculated free energies and entropies of mixing

Phase equilibria and calorimetry			Site-occupancy data		
Mole fraction $FeTiO_3$	ΔG_{mix} (kJ/mol)	ΔS_{mix}* [J/(mol·K)]	Mole fraction $FeTiO_3$	ΔS_{mix}**,† [J/(mol·K)]	ΔS_{mix}†,‡ [J/(mol·K)]
1	0	0	1	0	0
0.982	−2.314	1.310(0.2)	0.8630	10.81(63)	13.66(63)
0.957	−4.478	1.877(0.5)	0.7001	14.18(51)	16.49(51)
0.923	−6.705	2.789(0.8)	0.6094	16.14(50)	18.15(50)
0.887	−8.527	3.629(0.9)	0.4084	14.59(55)	15.94(55)
0.828	−10.723	4.924(1.6)	0.2402	9.91(27)	10.58(27)
0.751	−12.775	6.751(2.5)	0	0	0
0.701	−13.691	7.975(3.1)			
0.547	−14.644	11.384(3.6)			
0.330	−11.629	12.903(4.3)			
0	0	0			

* Errors (in parentheses) in ΔS_{mix} have been calculated from the error on the fit to ΔH_{mix}.
** Calculated ΔS_{mix} with site-occupancy data at 1573 K.
† The errors (in parentheses) represent the uncertainty in $S_{conf,ss}$, calculated assuming the maximum error (i.e., 0.024) in the Ti site-occupancy data, adjusting the other site occupancies according to compositional constraints, and assuming that Fe^{3+} is distributed equally on the A and B sublattices (see text for discussion).
‡ $S_{conf,ilm} = 3.30$ J/(mol·K) with site occupancy data at 1573 K and $S_{conf,ilm} = 0$ J/(mol·K).

$$S_{conf} = -R \sum_s \sum_i n_s x_{i,s}\ln x_{i,s} \quad (28)$$

where R is the gas constant, n_s is the number of sites, s, pfu, and $x_{i,s}$ is the mole fraction of atom i on site s. It is important to note that these configurational entropies represent maximum values in the sense that any short-range order on the A and B sublattices is neglected. The entropy of mixing is then defined as the difference between the configurational entropy of the solid solution, $S_{conf,ss}$, and the weighted sum of the standard-state configurational entropies of the end-members (i.e., $S_{conf,hem}$ and $S_{conf,ilm}$)

$$\Delta S_{mix} = S_{conf,ss} - x_{ilm}S_{conf,ilm} - (1 - x_{ilm})S_{conf,hem} \quad (29)$$

where x_{ilm} is the mole fraction of $FeTiO_3$ in the solid solution. Calculations of the entropies of mixing at various temperatures have been made for both standard states [Table 3 for $S_{conf,ilm} = 0$, Table 3 and Figure 6 for $S_{conf,ilm} = 3.3$ J/(mol·K)]. Figure 6 shows the change in the entropy of mixing as a function of annealing temperature and reflects the increase in order with decreasing annealing temperature for solid solutions with compositions from $x_{ilm} = 0.4$ to 0.85.

Calculation of entropies of mixing from ΔG_{mix} and ΔH_{mix}

The free energies of mixing determined from the phase equilibria data can then be used to calculate the entropy of mixing, ΔS_{mix}, with the relation

$$(-\Delta G_{mix} + \Delta H_{mix})/T = \Delta S_{mix}. \quad (30)$$

In this equation, the enthalpies of mixing are those determined experimentally (Eq. 1). Calculated entropies of mixing are listed in Table 7 and Figure 7. Values for ΔS_{mix}
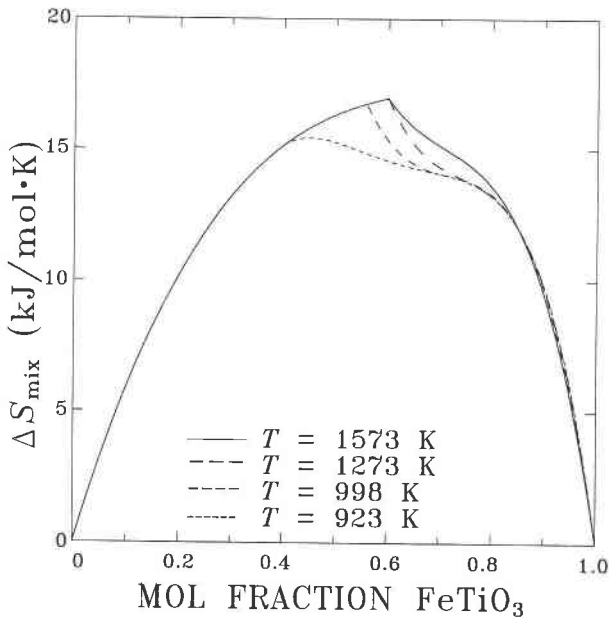
Fig. 6. Entropies of mixing calculated from site-occupancy data vs. mole fraction $FeTiO_3$ for different annealing temperatures and $S_{conf,ilm} = 3.3$ J/(mol·K). The decreasing entropy of mixing with decreasing temperature expresses the increase in cation order (see Table 1). The solid line represents data on samples quenched from 1573 K. The dashed lines represent entropies of mixing calculated for lower temperature anneals from 1273, 993, and 923 K (dash size decreases with decreasing temperature) (see Table 3).

Fig. 7. Solid circles represent the entropies of mixing calculated from site-occupancy data for $S_{conf,ilm} = 3.30$ J/(mol·K). The errors are represented by the symbol size. The open circles represent the entropies of mixing calculated with the free energies of mixing from our nonstoichiometric spinel model and the measured enthalpies of mixing. The error bars represent the uncertainty in this calculated entropy due to the error in the fit to the enthalpy of mixing. The open triangles represent the entropies of mixing, calculated using free energies of mixing from the empirical formulation of Ghiorso (1990), and our measured enthalpies of mixing. Errors bars for these data have been eliminated for clarity, but are the same as for the open circles.

(dashed curve in Fig. 7) have also been calculated using ΔG_{mix} (Ghiorso, 1990) and our experimentally determined enthalpies of mixing. The agreement between the two calculated entropies of mixing shows that determination of the free energies of mixing in Fe_2O_3-$FeTiO_3$ from our microscopically based model for the spinel solid solutions is in reasonable agreement with Ghiorso's empirical fit to the existing data in the hematite-ilmenite solid solution series. Ghiorso's empirical fit includes experimental data on both the order-disorder transition and the position of the solvus in the Fe_2O_3-$FeTiO_3$ solid solution series. In addition, both models show that the calculated entropies of mixing are significantly less positive than those inferred from measured cation distributions, especially for compositions with $x_{ilm} \geq 0.3$. This observation is also consistent with significant short-range order and may imply clustering of Ti in the Ti-rich B sublattice.

DISCUSSION

Solid solutions in the Fe_2O_3-$FeTiO_3$ system are characterized by two varieties of ordering: antiferromagnetic ordering of Fe in the temperature range of ~60–953 K, and chemical ordering of Fe^{2+} and Ti^{4+} between adjacent basal planes at temperatures between 873 and 1350 K (Ishikawa, 1958; Ishikawa and Akimoto, 1957; Ishikawa and Syono, 1963; Shirane et al., 1962). Magnetic ordering results from ferromagnetic intralayer magnetic interac-
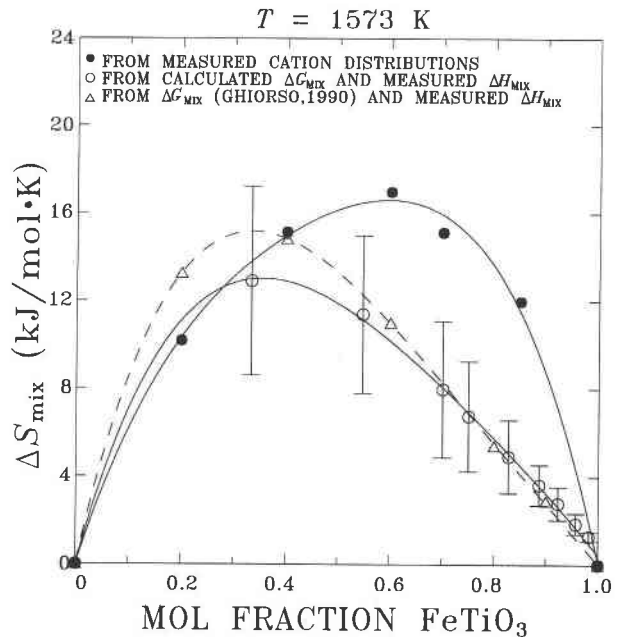
tions (i.e., magnetic moments within each sublattice are aligned parallel) and antiferromagnetic interlayer interactions between Fe atoms on the A and B sublattices (i.e., the magnetic moments of alternating A and B layers point in opposite directions). Chemical ordering arises from repulsive intralayer interaction and attractive interlayer interactions between Fe^{2+} and Ti^{4+}. In attempting to model the thermodynamic mixing properties by subregular and regular solution parameterizations, one loses the nature of these complex microscopic interactions that give rise to long-range and short-range ordering. CVM (cluster variation method) calculations (Burton, 1984; Burton and Kikuchi, 1984; Burton, 1985; Burton and Davidson, 1988) include the signs and magnitudes of these interactions and thus allow for more atomistically based descriptions of the thermodynamic properties of this solid solution series. They have been applied to carbonates (Capobianco et al., 1987) and to Fe_2O_3-$FeTiO_3$ (Burton, 1984; Burton, 1985; Burton and Davidson, 1988). The present data will be useful to constrain their parameters better, but such calculations are outside the scope of the current study.

Evidence for short-range ordering can be found for both magnetic and chemical ordering reactions. For example,

Grønvold and Samuelsen (1975) and Holland (1989) reported that hematite exhibits a long tail in the λ heat-capacity anomaly associated with magnetic ordering (transition temperature, T_c, = 955 K), suggesting significant incipient disorder in the magnetic spins even at 298 K. This disorder amounts to 17% of the maximum entropy that would be gained at T_c. Evidence of short-range chemical order can be seen for the range of compositions between x_{ilm} = 0.4 and 0.8. During quenching from temperatures above the order-disorder transition, both natural and synthetic solid solutions attempt to order. Local ordered regions nucleate and grow together. When two impinging ordered regions are in phase with one another, one large ordered region is formed. When they are out of phase, a compositionally distinct, cation-disordered twin-domain boundary (TDB) separates the two ordered regions. Such microscopic chemical domains and domain boundaries represent local variations in chemical order. These domains and domain boundaries, in turn, profoundly affect the magnetic ordering of solid solutions in this compositional range. Both reversed magnetization (Nord and Lawson, 1989, 1992; Hoffman, 1992; Lawson et al., 1981) and high coercivities (Brown et al., 1993) are intimately related to the development of TDBs during quenching through the order-disorder transition. The twin domain boundaries provide a second, more Fe-rich, magnetic phase that has a higher Curie temperature and causes the reversed magnetization seen in quenched natural and synthetic samples (Lawson, et al., 1981; Nord and Lawson, 1989; Nord and Lawson, 1992). In addition, Nord and Lawson (1992) proposed that when the chemical domain size is on the order of the magnetic domain size, the magnetic domain walls become pinned in the chemical domain walls. That gives rise to high coercivities in intermediate compositions and locally complex magnetic structure.

Evidence for short-range order can also be seen in the thermodynamic mixing properties of the $FeTiO_3$-Fe_2O_3 solid solution series. Measured enthalpies of mixing, ΔH_{mix}, can be interpreted as follows. The enthalpy of mixing for each solid solution composition arises from the sum of the atomic interaction energies in the crystal. In a solid solution series where both cation ordering and exsolution occur at varying temperatures, the measured mixing enthalpy can be broken down into two contributions: a positive mixing curve that will drive unmixing and a negative mixing curve that will drive ordering (Fig. 3). The functional form of the two opposite components of the total enthalpy depends on the strength of the positive and negative atomic interaction energies as a function of temperature and composition. One possible set of curves describing the two contributions to the measured enthalpy of mixing in Fe_2O_3-$FeTiO_3$ solid solutions is shown in Figure 3 (small dashed curves). As drawn, these curves suggest that in hematite-rich solid solutions, positive interaction energies dominate during initial substitution of $FeTiO_3$ into Fe_2O_3. Such behavior could arise from an increase in cation to cation repulsion across the

shared octahedral face due to increasing Ti^{4+} content and accompanying local displacements of the O ions to provide more shielding across the shared face. In ilmenite-rich solid solutions, negative ordering interactions dominate and reduce cation to cation repulsion across the shared face by placing Fe^{2+} and Ti^{4+} on separate sublattices. In the intermediate compositional range, as the Ti^{4+} content increases, the driving force for ordering increases, resulting in a progression from short-range ordering in the more Ti-poor solid solution to long-range ordering in the more Ti-rich solid solutions.

The implications of this work are important in terms of the development of thermodynamic models used to predict the activity-composition relationships at geologically relevant temperatures (~673–1173 K). This temperature range is precisely the range in which one would expect significant short-range and long-range ordering (both magnetic and chemical) to affect the thermodynamic properties. Paramagnetic to antiferromagnetic transitions in this temperature range occur for compositions from x_{ilm} = 0 to 0.4. Chemical ordering also occurs in this temperature range for compositions from x_{ilm} = 0.5 to 0.65 and possibly from as low as x_{ilm} = 0.2. This low compositional estimate is suggested by the high coercivities found in composition x_{ilm} = 0.2 and 0.4 (Brown et al., 1993). The complex temperature and compositional dependence of both the chemical and magnetic ordering reactions support use of such models as CVM, which include the atomic interactions that govern this complex T- and X-dependent behavior.

At first thought, one might be tempted to construct an empirical activity-composition model based on our enthalpies of mixing (Eq. 1), incorporating our excess entropies of mixing (open circles in Fig. 7). Algebraically, that could be done, but we believe it would have little, and only accidental, validity. Because the site occupancies and degree of short-range order depend strongly on temperature, it is highly likely that the entropy of mixing likewise has a strong temperature dependence. It seems unlikely that the activities depend on temperature and composition in a way that is simple enough to be modeled reliably by simple polynomials, especially in the T-X region of the order-disorder transition. The present study, in our interpretation, counsels caution in the indiscriminate use of ilmenite-spinel geothermobarometry for rocks, especially for lower grades of metamorphism, since extrapolation of higher temperature (>1100 K) activity data to the 700–1000 K range may be complicated by order-disorder phenomena.

The present data furnish a beginning to the quantification of these interactions, by providing constraints on both the enthalpies and entropies of mixing. However, the detailed temperature dependence of both long- and short-range order needs further study, and the further development of CVM or other structurally based models is necessary. The present calorimetric data refer to the enthalpy of mixing at room temperature of samples with a degree of short-range order and long-range order char-

acteristic of some higher temperature, but probably not preserving all the disorder of the high-temperature state. Thus, although the change in sign of ΔH_{mix} with composition and the smaller than configurational ΔS_{mix} are very suggestive of major short-range order, the data are insufficient to constrain quantitatively a microscopic mixing model as a function of both temperature and composition. The development of a complete microscopically based thermodynamic model for this system would require data on the in-situ state of ordering for each composition, heat-capacity data for each composition, and in-situ volume data as a function of composition. Once these data have been constrained, such a model could be constructed, and its free energies of mixing might then be used to parameterize more convenient empirical equations that would have the correct composition and temperature dependence.

ACKNOWLEDGMENTS

REFERENCES CITED

Andersen, D.J., and Lindsley, D.H. (1988) Internally consistent solution models for Fe-Mg-Mn-Ti oxides: Fe-Ti oxides. American Mineralogist, 73, 714–726.

Aragón, R., and McCallister, R.H. (1982) Phase and point defect equilibria in the titanomagnetite solid solution. Physics and Chemistry of Minerals, 8, 112–120.

Brown, N.E., Navrotsky, A., Nord, G.L., Jr., and Banerjee, S.K. (1993) Hematite-ilmenite (Fe₂O₃-FeTiO₃) solid solutions: Determinations of Fe-Ti order from magnetic properties. American Mineralogist, 78, 941–951.

Buddington, A.F., and Lindsley, D.H. (1964) Iron-titanium oxide minerals and synthetic equivalents. Journal of Petrology, 5, 310–357.

Burton, B.P. (1984) Thermodynamic analysis of the system Fe₂O₃-FeTiO₃. Physics and Chemistry of Minerals, 11, 132–139.

——— (1985) Theoretical analysis of chemical and magnetic ordering in the system Fe₂O₃-FeTiO₃. American Mineralogist, 70, 1027–1035.

Burton, B.P., and Davidson, P.M. (1988) Multicritical phase relations in minerals. In S. Ghose, J.M.D. Coey, and E. Salje, Eds., Structural and magnetic phase transitions in minerals, p. 60–90. Springer-Verlag, New York.

Burton, B.P., and Kikuchi, R. (1984) The antiferromagnetic transition in Fe₂O₃ in the single prism approximation of the cluster variation method. Physics and Chemistry of Minerals, 11, 125–131.

Capobianco, C., Burton, B.P., Davidson, P.M., and Navrotsky, A. (1987) Structural and Calorimetric studies of order-disorder in CdMg(CO₃)₂. Journal of Solid State Chemistry, 71, 214–223.

Ghiorso, M.S. (1990) Thermodynamic properties of hematite-ilmenite-geikielite solid solutions. Contributions to Mineralogy and Petrology, 104, 645–667.

Grønvold, F., and Samuelsen, E.J. (1975) Heat capacity and thermodynamic properties of α-Fe₂O₃ in the region 300 to 1050 K: Antiferromagnetic transition. Journal of the Physics and Chemistry of Solids, 36, 249–256.

Haggerty, S.E. (1976) Opaque mineral oxides in terrestrial igneous rocks. In Mineralogical Society of America Reviews in Mineralogy, 3, HG1–HG100.

Hoffman, K.A. (1992) Self-reversal of thermoremanent magnetization in the ilmenite-hematite system: Order-disorder, symmetry, and spin alignment. Journal of Geophysical Research, 97, 10883–10895.

Holland, T.J.B. (1989) Dependence of entropy on volume for silicate and oxide minerals: A review and a predictive model. American Mineralogist, 74, 5–13.

Ishikawa, Y. (1958) An order-disorder transformation phenomena in the FeTiO₃-Fe₂O₃ solid solution series. Journal of the Physical Society of Japan, 13, 828–837.

Ishikawa, Y., and Akimoto, S. (1957) Magnetic properties of the FeTiO₃-Fe₂O₃ solid solution series. Journal of the Physical Society of Japan, 12, 1083–1098.

Ishikawa, Y., and Syono, Y. (1963) Order-disorder transformation and reverse thermo-remanent magnetism in the FeTiO₃-Fe₂O₃ system. Journal of the Physics and Chemistry of Solids, 24, 517–528.

Kikuchi, R. (1977) The cluster variation method. Journal de Physique, colloque C7, suppl. 12, tome 38, 307–313.

Lawson, C.A., Nord, G.L., Jr., Dowty, E., and Hargraves, R.B. (1981) Antiphase domains and reverse thermoremanent magnetism in ilmenite-hematite minerals. Science, 213, 1372–1374.

Navrotsky, A. (1977) Progress and new directions in high temperature calorimetry. Physics and Chemistry of Minerals, 2, 89–104.

Nord, G.L., Jr., and Lawson, C.A. (1989) Order-disorder transition-induce twin domains and magnetic properties in ilmenite-hematite. American Mineralogist, 74, 160–176.

——— (1992) Magnetic properties of ilmenite₇₀-hematite₃₀: Effect of transformation-induced twin boundaries on magnetic stability and self-reversal. Journal of Geophysical Research, 97, 10897–10910.

O'Neill, H.St.C., and Navrotsky, A. (1984) Cation distributions and thermodynamic properties of binary spinel solid solutions. American Mineralogist, 69, 733–753.

Powell, R., and Powell, M. (1977) Geothermometry and oxygen barometry using coexisting iron-titanium oxides: A reappraisal. Mineralogical Magazine, 41, 257–263.

Schmalzried, H. (1983) Thermodynamics of compounds with narrow ranges of nonstoichiometry. Berichte der Bunsen-Gesellschaft für physikalische Chemie, 87, 726–733.

Senderov, E., Dogan, A.U., and Navrotsky, A. (1993) Nonstoichiometry of magnetite-ulvöspinel solid solutions quenched from 1300 °C. American Mineralogist, 78, 565–573.

Shirane, G., Cox, D.E., Takei, W.J., and Ruby, S.L. (1962) A study of the magnetic properties of the FeTiO₃-Fe₂O₃ system by neutron diffraction and the Mössbauer effect. Journal of the Physical Society of Japan, 17, 1598–1611.

Spencer, K.J., and Lindsley, D.H. (1981) A solution model for coexisting iron-titanium oxides. American Mineralogist, 66, 1189–1201.

Takayama-Muromachi, E., and Navrotsky, A. (1988) Energetics of compounds (A²⁺B⁴⁺O₃) with the perovskite structure. Journal of Solid State Chemistry, 72, 244–256.

Taylor, R.W. (1964) Phase equilibria in the system FeO-Fe₂O₃-TiO₂ at 1300 °C. American Mineralogist, 49, 1016–1030.

Thompson, J.B., Jr. (1969) Chemical reactions in crystals. American Mineralogist, 54, 341–375.

——— (1970) Chemical reactions in crystals: Corrections and clarifications. American Mineralogist, 55, 528–532.

Webster, A.H., and Bright, N.F.H. (1961) The system iron-titanium-oxygen at 1200 °C and partial oxygen pressures between 1 atm and 2 × 10⁻¹⁴ atm. Journal of the American Ceramic Society, 44, 110–116.

Wechsler, B.A., and Prewitt, C.T. (1984) Crystal structure of ilmenite (FeTiO₃) at high temperature and at high pressure. American Mineralogist, 69, 176–185.

Zhou, Z., Navrotsky, A., and McClure, D.S. (1993) Oxidation states of copper in lead borate (2PbO·B₂O₃) glass. Physics and Chemistry of Glasses, 34, 251–254.